# Consecutive Surface Reactions in Fully Developed Laminar and Turbulent Flow

R. W. LYCZKOWSKI, DIMITRI GIDASPOW, and C. W. SOLBRIG

Institute of Gas Technology, Chicago, Illinois

Consecutive reactions are frequently encountered in industrial practice (*1, 2*). The most common treatment involves the assumption of plug flow and negligible radial concentration gradients. For rapid surface reactions, these assumptions are not valid.

Exact solutions are obtained here for two consecutive first-order reactions occurring in a parallel plate reactor with one catalytic wall with fully developed laminar flow and in a tubular reactor with fully developed turbulent flow. Wall and mixing cup concentrations, selectivity, yield, and Nusselt number results are presented.

Local Nusselt numbers exhibit sharp discontinuities which lead one to conclude that two concentration boundary layers are formed. It was found that, in general, there is considerable departure from the yield and selectivity as predicted from the familiar plug flow solutions. Under some conditions, it is even possible to obtain mixing cup concentrations above those predicted by these analyses. Turbulence decreases the effective reaction rate coefficient by an order of magnitude as compared to laminar flow.

## BACKGROUND AND ASSUMPTIONS

Acrivos and Chambre (*14*) proposed integral equations to solve the isothermal first-order reversible problem as well as the irreversible consecutive surface reaction problem in the presence of a laminar boundary layer. To our knowledge, the only work concerned with essentially the same problem solved herein was considered by Hudson (*15*). He assumed uniform flow but allowed diffusion to occur in the radial direction. He used a change of variables which reduced his equations to a problem with sources in the fluid and boundary conditions of the third type. His concentration profiles results are limited but qualitatively similar to those found here. Wissler and Schechter (*16*) considered the consecutive reaction to occur in the fluid stream only (homogeneous reaction).

For both of the problems under consideration, the following reaction

$$\alpha A \xrightarrow{k_A} \beta B \xrightarrow{k_B} \text{products} \qquad (1)$$

is occurring only on the periphery of the reactor. It is assumed that both steps of the reaction are irreversible and first order in each species and that any heat liberated (or absorbed) in the course of the reaction is removed (or supplied) through the walls which are composed of a good heat conductor, such as alumina or copper. Species A is assumed to control the first reaction. This is possible if it is highly diluted. If A is present in small quantities, B is also present in small quantities when none is fed into the reactor, and it will control the second step. Multicomponent effects vanish when a large amount of inert, such as air, is present. In addition, the usual Graetz assumptions are invoked for the flowing fluid and may be found in (*3*) and (*17*). Experimental verification of the assumptions may be found in (*18*).

## LAMINAR FLOW BETWEEN PARALLEL PLATES

### Analytical Statement of the Problem

In this geometry the reaction shown by Equation (1) occurs at the bottom wall, $\xi = -1$ only. The governing partial differential equation together with the boundary conditions (B.C.) appropriate to the geometry in dimensionless form are

$$D^* (1 - y^2) \frac{\partial C_B}{\partial x} = \frac{\partial^2 C_B}{\partial y^2} \qquad (2)$$

$$\text{I.C.:} \quad C_B (0, y) = 0 \qquad (3)$$

$$\text{B.C. 1:} \quad \frac{\partial C_B}{\partial y} (x, +1) = 0 \qquad (4)$$

$$\text{B.C. 2:} \quad \frac{\partial C_B}{\partial y} (x, -1) = -D^* K_A C_A (x, -1) + K_B C_B (x, -1) + K_B C_B{}^0 \qquad (5)$$

If $K_B = 0$, the problem reduces to the one solved by Lyczkowski et al. (*19*), and then a constant flux kernel is required. In that work, for the temperature problem, the reactor had to be adiabatic. Now we may allow heat to leave the system. Assuming that the catalytic wall is thin enough for the temperature distribution to be approximated by a linear drop through the plate (caused by conduction) and an additional linear drop through the outside (caused by a film resistance), new symbols may replace the present ones and the heat transfer problem is solved. Therefore, if one replaces $D^*$ by $N_{Le}$, $C_B$ by $\overline{T}$, $C_B{}^0$ by $\overline{T}_{i,s}$ and $K_B$ by $N_{Bi}$ in Equations (2) to (5), we obtain the solution to the temperature problem associated with the consecutive reaction $\alpha A \rightarrow \beta B$. The additional assumptions required are stated in reference (*19*).

### Solution by Duhamel's Theorem

To solve the problem, the expression for $K_A C_A (x, -1)$ is required. This has been obtained by Solbrig and Gidaspow (*4*) and is directly usable in the second boundary condition, because their solution for $C_A$ is identical to the one required for this problem. This quantity is expressed as an infinite series. It will be convenient to rewrite Equation (5) as

$$\frac{\partial C_B}{\partial y} (x, -1) - K_B C_B (x, -1) = f(x) \qquad (6)$$

where

$$f(x) = -D^* \sum_{m=1}^{\infty} \gamma_m{}^2 \beta_m{}^2 e^{-\beta_m{}^2 x} + K_B C_B{}^0 \qquad (7)$$

Now the problem is solvable by the use of Duhamel's theorem. For reference use, we state the form of the theorem which we used in this study

$$C_B(x, y) = C_{B_1}(0^+, y) \cdot f(x) + \int_0^x \frac{\partial}{\partial x} [C_{B_1} (x - X, y)] f(X)\, dX \qquad (8)$$

where $C_{B_1} (x, y)$ is the solution to the problem when $f(x) \equiv 1$, i.e., unit surroundings. The presence of the first term is explained in reference *19*. The solution for $C_{B_1}$ is

R. W. Lyczkowski is with Goodyear Atomic Corporation, Piketon, Ohio. C. W. Solbrig is with Idaho Nuclear Corporation, Idaho Falls, Idaho.

$$C_{B_1}(x, y) = \frac{1}{K_B}\left[\sum_{j=1}^{\infty} \gamma_j \psi_j(y)\, e^{-\beta_j^2 x/D^*} - 1\right] \tag{9}$$

The eigen-parameters for $C_{B_1}$ are those associated with the Graetz problem having boundary conditions of the third type and may be found in (*4*) or, more completely in (*13*). They are tabulated for other flow regimes and geometries of interest in (*3-13*).

Now the point concentration, $C_B$ may be constructed by elementary differentiation of Equation (9) and integration of Equation (8). The final result is

$$C_B{}^0 + C_B(x, y) = \frac{D^*}{K_B}\left[\sum_{m=1}^{\infty} \gamma_m{}^2 \beta_m{}^2 e^{-\beta_m{}^2 x}\right]\left[1 - \sum_{j=1}^{\infty} \gamma_j \psi_j(y)\right] + \frac{D^*}{K_B}\sum_{m=1}^{\infty}\sum_{j=1}^{\infty} \gamma_j \gamma_m{}^2 \psi_j(y)\, \beta_j{}^2 \left[\frac{e^{-\beta_m{}^2 x} - e^{-\beta_j{}^2 x/D^*}}{\left(\frac{\beta_j}{\beta_m}\right)^2 - D^*}\right] + C_B{}^0 \sum_{j=1}^{\infty} \gamma_j \psi_j(y)\, e^{-\beta_j{}^2 x/D^*} \tag{10}$$

The wall concentration is obtained by setting $y = -1$ in Equation (10) and replacing $\gamma_j \psi_j(-1)$ by $\gamma_j{}^2 \beta_j{}^2$. The gradient may be obtained directly from the boundary condition, Equation (6). The mixing cup concentration is defined as

$$C_{B_m}(x) = \int_{-1}^{+1} (1 - y^2)\, C_B(x, y)\, dy \Big/ \int_{-1}^{+1} (1 - y^2)\, dy \tag{11}$$

and its expression is

$$C_{B_m} + C_B{}^0 = \frac{3}{4}\frac{D^*}{K_B}\sum_{j=m=1}^{\infty}\sum^{\infty} \gamma_m{}^2 \beta_j{}^2 \gamma_j{}^2 \left[\frac{e^{-\beta_m{}^2 x} - e^{-\beta_j{}^2 x/D^*}}{\left(\frac{\beta_j}{\beta_m}\right)^2 - D^*}\right] + \frac{3}{4} C_B{}^0 \sum_{j=1}^{\infty} \gamma_j{}^2 e^{-\beta_j{}^2 x/D^*} \tag{12}$$

Whenever $D^* = \left(\frac{\beta_j}{\beta_m}\right)^2$, we must replace the bracketed quantity by

$$\frac{\beta_m{}^4}{\beta_j{}^2} \cdot x \cdot e^{-\beta_m{}^2 x} \text{ or by } \frac{\beta_m{}^2}{D^*} \cdot x \cdot e^{-\beta_m{}^2 x}$$

The solution was verified as being correct for wall, mixing cup concentrations, gradient, and Nusselt numbers by considering the case $K_B \to 0$. We ran $K_A = 1.0$ and $K_B = 0.001$ and found that these results agreed with those of Lyczkowski et al., (*19*) to within six significant figures in concentrations and three in Nusselt numbers, which are much more sensitive to error.

Let us now turn to some results of our computations. Figure 1 shows mixing cup results for $K_A/K_B D^* = 1$ and $C_B{}^0 = 0$. The distance parameter used is the one that results from a one dimensional plug flow analysis. Plots of our solution using this distance will reveal departure from "ideal flow." The curve labeled "plug flow" is the solution from the classical one-dimensional analysis and may be found, for example, in Levenspiel (*1*) or Aris (*2*). The effect of diffusion is clearly evident. The yield decreases as $D^*$ increases for constant $K_A$. As $K_A$ becomes larger, there is further departure from ideal flow.

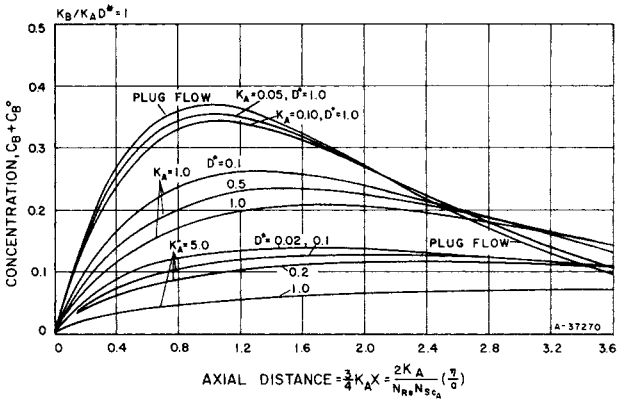


**Fig. 1. Laminar flow between parallel plates: effect of diffusivity ratio on mixing cup concentration profiles, $C_B{}^0 = 0$.**

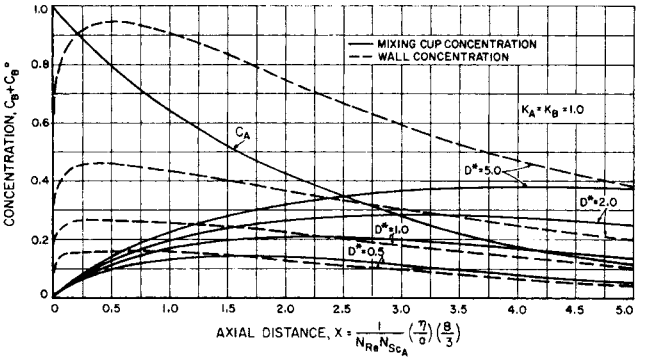


**Fig. 2. Laminar flow between parallel plates: effect of diffusivity ratio on wall and mixing cup concentration profiles, $K_A = K_B = 1.0$.**

An interesting and unexpected result occurred which considerably reduced the number of graphs to be plotted. It was found that, if the numerical values of $K_A$ and $K_B$ are interchanged but the ratio of $K_B/K_A D^*$ is kept the same, numerical results for the two curves are identical for all practical purposes. For example, in Figure 1, results for $K_A = 1$, $K_B = 0.5$, and $D^* = 0.5$ are identical to $K_A = 0.5$, $K_B = 1.0$, and $D^* = 2.0$. The reason for this coincidence is not obvious from the solution, Equation (12).

Figure 2 shows typical wall and mixing cup concentrations as being affected by $D^*$ for equal $K_A$ and $K_B$. As $D^*$ is increased, the yield increases. Wall concentrations are the most sensitive to the ratio and reach very high maxima in comparison to the mixing cup maxima. In addition, they occur for much smaller axial distance. Invariably, the wall and mixing cup curves cross over and it is at these values of the dimensionless distance that the Nusselt number goes through a discontinuity. (More will be said about this later.) Up to the point of equality, wall concentrations are higher than the mean, and after, they are lower. The mixing cup concentration of species $A$ is not affected by $D^*$ for constant $K_A$ and is plotted for reference purposes as $C_A$.

### Laminar Nusselt Numbers

We define the general Nusselt number for mass transfer in the following manner

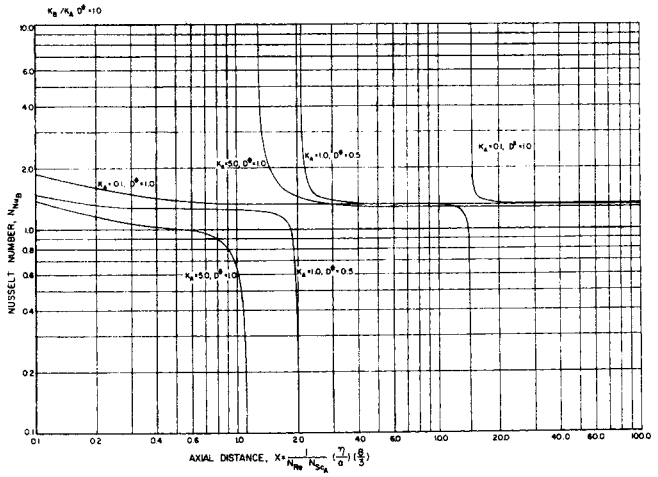


Fig. 3. Laminar flow between parallel plates: Nusselt numbers, $C_B^\circ = 0$.

$$N_{Nu_i} = \frac{k_{gi} l}{D_{ie}} = \frac{\dfrac{\partial C_i}{\partial \vec{n}}(x, r_s)}{C_{im} - C_{iw}} \tag{13}$$

Where $l$ is a characteristic dimension, $\vec{n}$ is an outward normal to $r_s$, the surface upon which the reaction is occurring. $C_{i_w}$ is an abbreviation for $C_i(x, r_s)$. For this problem, $l = a$, $\vec{n} = +y$, and $r_s = -1$, and we deal with species $B$. Figure 3 shows the results for the case when $C_B{}^0 = 0$. In every case, the entrance region Nusselt numbers appear to level off but, after some distance, there is a sharp discontinuity where the values descend to $-\infty$ and come back down from $+\infty$.

The reason for the discontinuity seems clear if one considers the existence of two concentration boundary layers for species $B$. When one enters the reactor with no species $B$, its net diffusion at first is away from the wall, resulting in a boundary layer which grows until there is a maximum in the mixing cup concentration. It is right at this maximum that the wall concentration equals the mixing cup and the net diffusion of species $B$ reverses toward the wall. This existence of two concentration boundary layers explains the reason for two Nusselt number entrance regions. It should be pointed out that the derivation of B.C. 2 in Equation (5) considers the diffusional fluxes both toward and away from the wall. The net diffusional fluxes, however, are as have been described. Consequently, species $B$ is always having a chance to react at the wall in both of the boundary layers, and this effect is automatically accounted for in the boundary condition.

The value for fully developed Nusselt number $N_{Nu_B}$ corresponds very closely in value to the one obtained previously (*4, 13*) for $N_{Nu_A}$ for corresponding $K_A$ and is not affected greatly by $D^*$ or $K_A$. For instance, when $K_A = 0.05$ the values for fully developed $N_{Nu_B}$'s are 1.345, 1.347, and 1.362 for $D^*$'s of 0.5, 1.0,and 2.0, respectively, while $N_{Nu_A}$ is 1.3412. These values indicate that the boundary condition does not have much effect on fully developed Nusselt numbers and contrast with the fully developed Nusselt numbers of reference *19* which tend to zero as $D^*$ becomes large.

## TURBULENT FLOW IN A ROUND TUBE

### Analytical Statement and Solution by Duhamel's Theorem

In a manner entirely analogous to the preceding, we proceed to derive similar results for turbulent flow in a tube. Wissler and Schechter's (3) eigenfunction solution

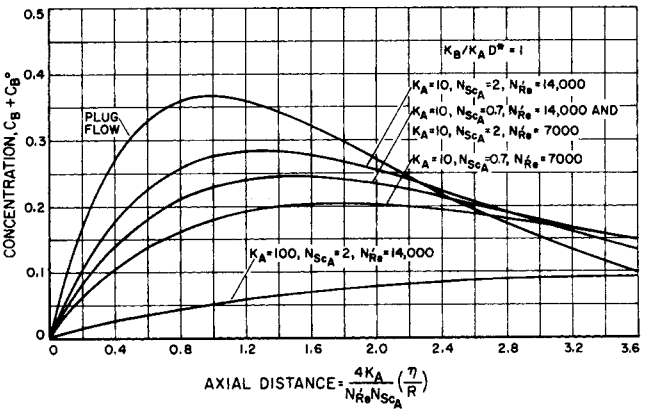


Fig. 4. Turbulent flow in a tube: representative mixing cup concentration profiles, $C_B^\circ = 0$.

is used to derive the numerical results for this geometry. In dimensionless form, the governing partial differential equation and appropriate boundary conditions are

$$N_{Sc_B} u^+(r^+) \frac{\partial C_B}{\partial z} = \frac{R^+}{r^+} \frac{\partial}{\partial r^+} \left[ r^+ \left( 1 + \frac{D_t(r^+)}{D_{Be}} \right) \frac{\partial C_B}{\partial r^+} \right] \tag{14}$$

$$\text{I.C.:} \quad C_B(r^+, 0) = 0 \tag{15}$$

$$\text{B.C. 1:} \quad \frac{\partial C_B}{\partial r^+}(0, z) = 0 \tag{16}$$

$$\text{B.C. 2:} \quad -\frac{\partial C_B}{\partial r^+}(R^+, z) = \frac{K_B}{R^+} C_B(R^+, z) + f(z) \tag{17}$$

where

$$f(z) = -\frac{D^* K_A}{R^+} \sum_{n=1}^{\infty} C_n \psi_n(R^+) e^{-2\beta_n^2 \frac{z}{N'_{Re}}} + \frac{K_B}{R^+} C_B \tag{18}$$

The infinite series in B.C. 2 is the wall concentration for species $A$ taken from Wissler and Schechter (3) where the eigenvalues and eigenparameter are also tabulated. The plussed symbols are "parameter coordinates." To convert to the ordinary dimensionless coordinate $\bar{r}$ (which must be done for the Nusselt number), multiply $r^+$ by $R^+$.

By setting $f(z) \equiv 1$, we obtain the kernel solution for use in Duhamel's theorem, Equation (8):

$$C_{B_1}(r^+, z) = \frac{R^+}{K_B} \left[ \sum_{j=1}^{\infty} C_j \psi_j(r^+) e^{-2\beta_j^2 \frac{z}{N'_{Re}}} - 1 \right] \tag{19}$$

After differentiating Equation (19) and integrating as shown in Equation (8), we obtain the point concentration as

$$C_B(r^+, z) + C_B{}^0 = D^* \frac{K_A}{K_B} \sum_{n=1}^{\infty} C_n \psi_n(R^+) e^{-2\beta_n^2 \frac{z}{N'_{Re}}} \left[ 1 - \sum_{j=1}^{\infty} C_j \psi_j(R^+) \right] + D^* \left( \frac{K_A}{K_B} \right) \sum_{j=1}^{\infty} \sum_{n=1}^{\infty} C_j \psi_j(r^+)$$

$$C_n \psi_n (R^+) \beta_j^2 \left[ \frac{e^{-2\beta_n^2 \frac{z}{N'_{Re}}} - e^{-2\beta_j^2 \frac{z}{N'_{Re}}}}{\beta_j^2 - \beta_n^2} \right] + C_B{}^0 \sum_{j=1}^{\infty} C_j \psi_j (r^+) e^{-2\beta_j^2 \frac{z}{N'_{Re}}} \quad (20)$$

The mixing cup concentration is obtained by the definition

$$C_{Bm} = \frac{1}{\pi R^2 U} \int_0^R 2\pi r u C_B(r, z)\, dr = \frac{2}{(R^+)^2 U^+} \int_0^{R^+} r^+ u^+ C\,(r^+, z)\, dr^+ \quad (21)$$

When Equation (20) is substituted into this definition, the result is:

$$C_{Bm} + C_B{}^0 = \frac{4}{N'_{Re} R^+} \left\{ D^* \frac{K_A}{K_B} \sum_{j=n=1}^{\infty} \sum^{\infty} \beta_j^2 C_j^2 N_j C_n \psi_n(R^+) \left[ \frac{e^{-2\beta_n^2 \frac{z}{N'_{Re}}} - e^{-2\beta_j^2 \frac{z}{N'_{Re}}}}{\beta_j^2 - \beta_n^2} \right] + C_B{}^0 \sum_{j=1}^{\infty} C_j^2 N_j e^{-2\beta_j^2 \frac{z}{N'_{Re}}} \right\} \quad (22)$$

Whenever $\beta_j^2 = \beta_n^2$, replace the bracketed term by

$$2 \frac{z}{N'_{Re}} e^{-2\beta_j^2 \frac{z}{N'_{Re}}}.$$

We present results in Figure 4 for the same case as in laminar flow, i.e., $K_B/K_A\, D^* = 1$. The dimensionless distance again corresponds to the plug flow coordinate. By comparing Figures 4 and 1, it is obvious that the hydrodynamics has intervened to such an extent that about an order of magnitude increase in the reaction rate constant $K_A$ left the results almost the same. It was found that the cases of $K_A = K_B = 10$, $N_{Sc_A} = N_{Sc_B} = 0.7$, and $N'_{Re} = 14{,}000$ and $K_A = K_B = 10$, $N_{Sc_A} = N_{Sc_B} = 2$ and $N'_{Re} = 7{,}000$ were identical for all practical purposes.

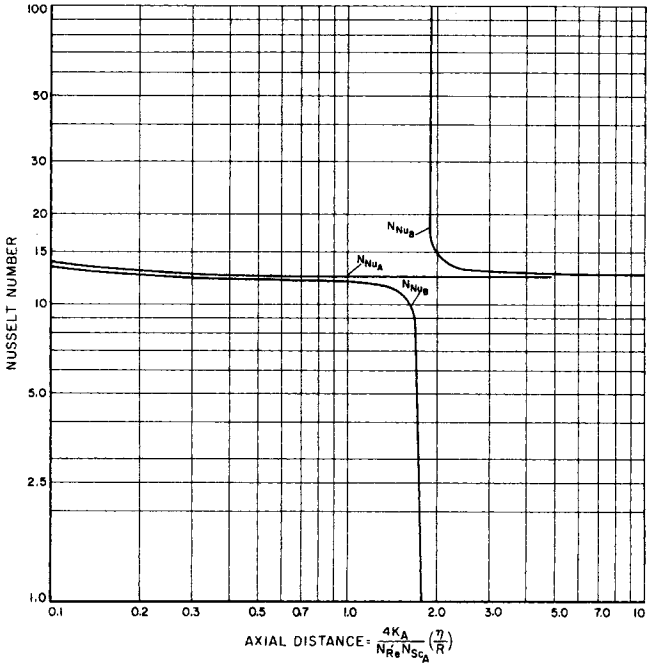


Fig. 5. Turbulent flow in a tube: Nusselt numbers, $K_A = K_B = 10$, $D^* = 1.0$, $N_{Sc_A} = N_{Sc_B} = 0.7$, $N'_{Re} = 7{,}000$, $C_B = 0$.

### Turbulent Nusselt Numbers

In Equation (13) we replace $l$ by $R$, $x$ by $z$, $\vec{n}$ by $-\vec{r}$ and $r_s$ by 1 and substitute the quantities calculated from the solution. We defined a similar Nusselt number for species $A$ and calculated the fully developed values from the eigenvalues in Wissler and Schechter (3).

We did this so we could derive an approximate Dittus-Boelter relation to correlate these values. We found that in the range Wissler and Schechter worked ($N'_{Re}$ from 7,000 to 14,000), the fully developed values correlate with

$$N_{Nu_A} \text{ fully developed} \approx 0.051\, N'_{Re}{}^{0.64}\, N_{Sc_A}{}^{0.44} = \frac{k_{gA} R}{D_{Ae}} \quad (23)$$

Solbrig and Gidaspow (17) found a 0.69 to 0.77 power on the Reynolds number for Schmidt numbers from 1 to 0.2 and a 0.61 to 0.69 power on the Schmidt number for Reynolds number from 30,000 to 70,000 for turbulent flow between parallel plates with reaction on one wall.

Figure 4 shows our results plotting $N_{Nu_A}$ and $N_{Nu_B}$ for the parameters indicated. In the entrance region both curves are similar, with $N_{Nu_B}$ being slightly lower. It appears that the curve is fully developed at a dimensionless distance of 0.7, but the second boundary layer then begins to form and the Nusselt number goes through the same type of discontinuity as was found for laminar flow.

### Selectivity

It is extremely useful to have criteria for the actual reactor design. We want maximum selectivity and as high a yield as possible. The definition of selectivity as used here is the same as used by Spielman (20) and is the ratio of the mole fraction of desired product $X_B$ to the mole fraction of all products $X_B + X_C$. Actually $X_B + X_C$ is the conversion of species $A$, $1 - X_A$. So our selectivity definition becomes

$$\text{Selectivity} = \frac{\text{Fraction of desired product, } B}{\text{Conversion of } A}$$

We plot this quantity versus the total yield $X_B$ in Figure 6. Molecular or eddy diffusion or both considerably lower

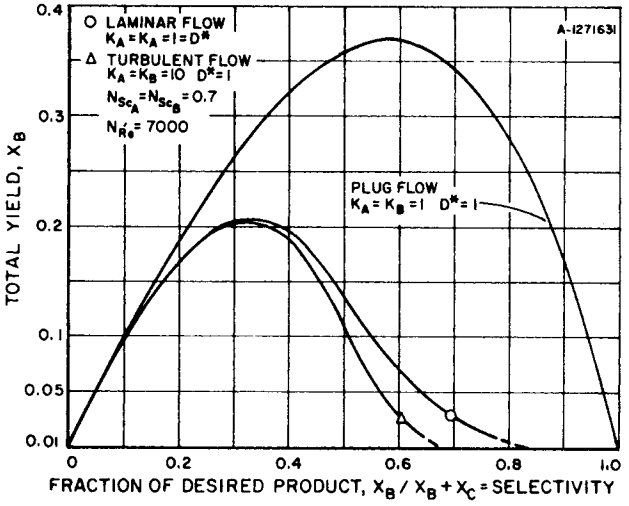


Fig. 6. Comparison of yield and selectivity for laminar, turbulent, and plug flows, $C_B{}^\circ = 0$.

the selectivity and the yield as compared to plug flow because they present a resistance for species to react at the catalytic wall which is not present in the plug flow analysis. Charts of this kind are useful because they tell one what happens if one wants to sacrifice yield for selectivity. Knowing the yield immediately tells the designer what flow conditions are required for a certain reactor length or, if flow is fixed, what the length of the reactor should be. In the limit, at $\eta = 0$ the selectivity for the plug flow reactor is one; with the presence of diffusion, the limit appears to be less than one.


## ACKNOWLEDGMENT

The investigation was supported through the basic research program of the Institute of Gas Technology. Partial support was provided to Mr. Lyczkowski by an award of a Natural Gas Supplymen's Fund Fellowship.


## NOTATION

$a$ = one half the distance between the catalytic and noncatalytic plate, ft.

$C_A$ = dimensionless concentration of controlling reactant species, $\rho_A/\rho_{A0}$

$C_B$ = dimensionless concentration of intermediate reactant species, $\frac{\rho_B - \rho_{B0}}{\rho_{A0}}\left(\frac{\alpha}{\beta}\right)\left(\frac{M_A}{M_B}\right)$

$C_B{}^0$ = dimensionless entering concentration of intermediate reactant species, $\frac{\rho_{B0}}{\rho_{A0}}\left(\frac{\alpha}{\beta}\right)\left(\frac{M_A}{M_B}\right)$

$C_i$ = coefficient for the $i^{th}$ mode

$C_P$ = heat capacity at constant pressure, B.t.u./(lb.)(°F.)

$D_{ie}$ = effective diffusivity of species $i$ in a mixture, sq.ft./hr.

$D^*$ = diffusivity ratio of controlling reactant and intermediate, $D_{Ae}/D_{Be} = N_{ScB}/N_{ScA}$

$D_t$ = eddy diffusivity, sq.ft./hr.

$h$ = overall heat transfer coefficient = $1 \Big/ \left(\frac{t}{k_s} + \frac{1}{h_0}\right)$, B.t.u./(hr.)(sq.ft.)(°F.)

$h_0$ = outside heat transfer coefficient, B.t.u./(hr.)(sq.ft.)(°F.)

$-\Delta H$ = exothermic heat of reaction, B.t.u./lb.

$K_{Ei}$ = effective dimensionless reaction rate constant for species, $i = k_{Ei}l/D_{ie}$

$K_i$ = dimensionless reaction rate constant for species, $i = k_{il}/D_{ie}$

$k$ = thermal conductivity of flowing fluid, B.t.u./(hr.)(°F.)(ft.)

$k_i$ = reaction rate coefficient for species $i$, ft./hr.

$k_{gi}$ = mass transfer coefficient for species $i$, ft./hr.

$k_{Ei}$ = effective reaction rate constant = $1/(1/k_i + 1/k_{gi})$, ft./hr.

$k_s$ = thermal conductivity of catalytic wall, B.t.u./(hr.)(°F.)(ft.)

$l$ = characteristic length, ft.

$M_i$ = molecular weight of species $i$, lb./lb.-mole

$\vec{n}$ = an outward drawn normal, ft.

$N_{Bi}$ = Biot number, $hl/k$

$N_i$ = square of the norm of $\psi_i$

$N_{Le}$ = Lewis number, $D_{Ae}/\alpha$

$N_{Nui}$ = Nusselt number for species $i$, $N_{Nui} = k_{gi}l/D_{ie}$ for mass transfer; $N_{Nu} = hl/k$ for heat transfer

$N_{Pe}$ = Peclet number, $4aU/D_{Ae}$ or $4aU/\alpha$

$N_{Pr}$ = Prandtl number, $\mu C_p/k$

$N_{Re}$ = Reynolds number for parallel plates, $4aU\rho/\mu$

$N'_{Re}$ = Reynolds number for tube, $2RU\rho/\mu = 2R^+U^+$

$N_{Sci}$ = Schmidt number of species $i$, $\mu/\rho\, D_{ie}$

$r$ = radial coordinate for the tube, ft.

$\bar{r}$ = dimensionless radial coordinate, $r/R$

$r^+$ = dimensionless radial coordinate, $r\sqrt{\tau_w\rho}\,\rho/\mu$

$\mathbf{r}_s$ = vector to reactive surface, ft.

$R$ = inside radius of the tube, ft.

$R^+$ = dimensionless inside radius of the tube, $R\sqrt{\tau_w\rho}\,\rho/\mu$

$\bar{T}$ = dimensionless temperature, $\dfrac{T - T_i}{\dfrac{(-\Delta H)\rho_{A0}}{C_P\rho}} = \dfrac{T - T_i}{T_{AD}}$

$\bar{T}_{i,s}$ = $(T_i - T_s)/T_{AD}$

$T$ = temperature, °F.

$t$ = catalytic wall thickness, ft.

$u$ = velocity in the direction of flow, ft./hr.

$u^+$ = dimensionless velocity in the direction of flow, $u/\sqrt{\tau_w\rho}$

$U$ = spatial average velocity, ft./hr.

$U^+$ = dimensionless spatial average velocity, $U/\sqrt{\tau_w\rho}$

$x$ = dimensionless coordinate parallel to flow, $\eta \Big/ \frac{3}{2}\frac{Ua^2}{D_{Ae}} = \frac{1}{N_{Re}\,N_{ScA}}\left(\frac{\eta}{a}\right)\left(\frac{8}{3}\right)$ for mass transfer; and $\eta \Big/ \frac{3}{2}\frac{Ua^2}{\alpha} = \frac{1}{N_{Re}\,N_{Pr}}\left(\frac{\eta}{a}\right)\left(\frac{8}{3}\right)$ for heat transfer

$y$ = dimensionless coordinate parallel to flow, $\xi/a$

$z$ = dimensionless coordinate parallel to flow, $\eta/R$

### Greek Letters

$\alpha$ = stoichiometric coefficient; thermal diffusivity, $\dfrac{k}{\rho C_p}$ sq.ft./hr.

$\beta_i$ = eigenvalue for $i^{th}$ mode

$\gamma_i$ = normalized coefficient for $i^{th}$ mode

$\eta$ = spatial coordinate parallel to flow direction, ft.

$\mu$ = absolute viscosity, lb./(ft.)(hr.)

$\xi$ = spatial coordinate perpendicular to the flow direction and the catalytic plate, ft.

$\rho$ = total mass density, $\sum_i^N \rho_i$, lb./cu.ft.

$\rho_i$ = mass concentration of species $i$, lb./cu.ft.

$\tau_w$ = wall shear stress, $4\,\mu U/R$, lb./(sq.ft.)(hr.)

$\psi_i$ = normalized eigenfunction for $i^{th}$ mode

### Subscripts

$i$, 0 = based upon entering reactor conditions

$m$ = mixing cup

$s$ = surroundings temperature

$w$ = catalytic wall

## LITERATURE CITED


1. Levenspiel, Octave, "Chemical Reaction Engineering," John Wiley, New York (1962).
2. Aris, Rutherford, "Introduction to the Analysis of Chemical Reactors," Prentice-Hall, Englewood Cliffs (1965).
3. Wissler, E. H., and R. S. Schechter, *Chem. Eng. Sci.*, **17**, 937 (1962).
4. Solbrig, C. W., and Dimitri Gidaspow, *Can. J. Chem. Eng.*, **45**, 35 (1967).
5. Predvoditelev, A. S., "Combustion of Carbon," Moskva Akad. Nauk (1949).
6. Van der Does de Bye, J. A. W., and J. Schenk, *Appl. Sci. Res.*, **A3**, 308 (1952).
7. Schenk, J., and J. M. Dumore, *ibid.*, **A4**, 39 (1953).
8. ———, and H. L. Beckers, *ibid.*, **A4**, 405 (1954).
9. ———, *ibid.*, **A5**, 241 (1955).

10. ———, and J. V. Laar, *ibid.*, **A7**, 449 (1958).
11. Sideman, S., D. Luss, and R. E. Peck, *ibid.*, **A41**, 157 (1964/65).
12. Hsu, C.-J., and Huang, C.-J., *Chem. Eng. Sci.*, **21**, 209 (1966).
13. Solbrig, C. W., Ph.D. thesis, Illinois Institute of Technology, Chicago (1966).
14. Acrivos, Andreas, and P. L. Chambre, *Ind. Eng. Chem.*, **49**, 1025 (1957).
15. Hudson, J. L., *AIChE J.*, **11**, 943 (1965).
16. Wissler, E. H., and R. S. Schechter, *Appl. Sci. Res.*, **A10**, 198 (1961).
17. Solbrig, C. W., and Dimitri Gidaspow, *Intern. J. Heat Mass Transfer*, **11**, 155 (1968).
18. Kulacki, F. A., and Dimitri Gidaspow, *Can. J. Chem. Eng.*, **45**, 72 (1967).
19. Lyczkowski, R. W., Dimitri Gidaspow, and C. W. Solbrig, *Chem. Eng. Progr. Symp. Ser.*, No. 77, **63**, 1 (1967).
20. Spielman, Maurice, *AIChE J.*, **10**, 496 (1964).

# Three-Dimensional Light Intensity Distribution Model for an Elliptical Photoreactor

**WILLIAM J. ZOLNER III and JOHN A. WILLIAMS**

**Northeastern University, Boston, Massachusetts**

Matsuura, Cassano, and Smith (*11*) and Matsuura and Smith (*12*) proposed a diffuse light model to represent the distribution of light intensity within an elliptical reflector-tubular photoreactor. The model was selected because it represented the author's intuitive concept of the light distribution resulting from an imperfect reflector better than did the classical radial distribution model (*2, 3, 4, 5, 6, 7, 14*). Data presented by Jacob and Dranoff (*8*) support the view that a diffuse model might be more appropriate than a radial model in some cases.

It is the purpose of this note to propose a three-dimensional diffuse model to represent the light distribution in an elliptical photoreactor. The model contains two adjustable parameters whose values can be estimated from experimental data. It is shown that the diffuse light model of Smith and coworkers represents a limiting case of the three-dimensional model when one of its adjustable parameters assumes an extreme value.

## THE MODEL

This model, shown schematically in Figure 1, consists of two concentric right cylinders; the inner cylinder of radius $R_r$ represents the reactor tube while the outer cylinder of radius $R_1$ represents the light source. The light source cylinder is assumed to be a continuous sheath of light of uniform intensity.

Following the methods for point kernel integration, similar to those used in nuclear radiation shielding problems (*9*), the light intensity at any point in the reactor is given by

$$I(r, z') = \int_0^{z'} \int_0^{2\pi} \frac{S_0 R_1 e^{-\mu x}\, d\psi dz}{R_1^2 + r^2 + z^2 - 2R_1 r\cos\psi} + \int_0^{L-z'} \int_0^{2\pi} \frac{S_0 R_1 e^{-\mu x}\, d\psi dz}{R_1^2 + r^2 + z^2 - 2R_1 r\cos\psi} \quad (1)$$

The model can be used to compute the radial and axial variation of intensity at any point within the reactor. It was assumed that no reflection or refraction occurs at the wall, that the light is monochromatic, and that the medium

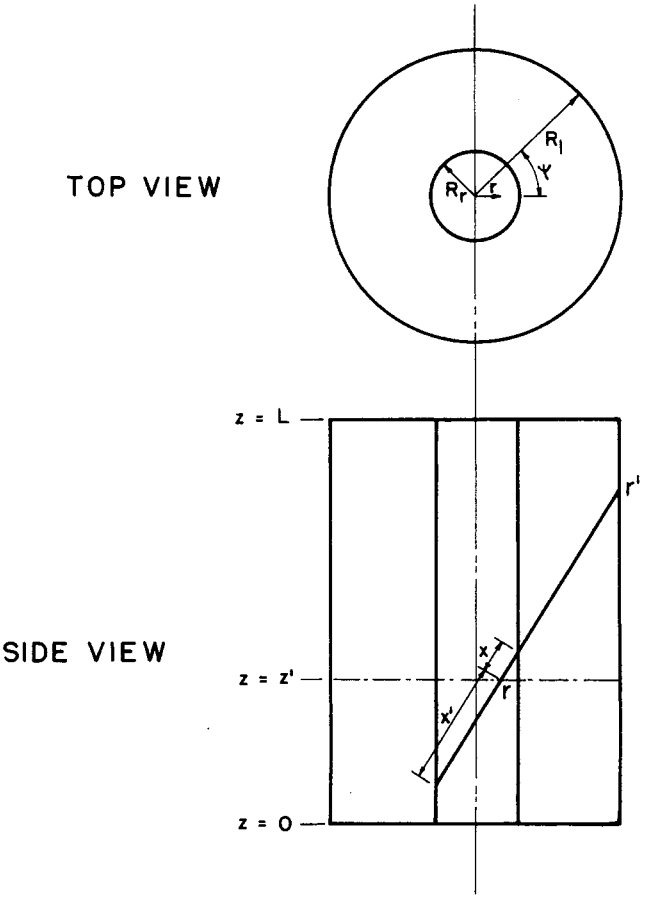


Fig. 1. Schematic of three-dimensional light distribution model.